

## The Mu2e experiment

---

**Stefano Di Falco<sup>a,\*</sup> for the Mu2e collaboration\***

<sup>a</sup>*INFN Pisa,*

*Largo B. Pontecorvo 3, Pisa, Italy*

*E-mail: [stefano.difalco@pi.infn.it](mailto:stefano.difalco@pi.infn.it)*

The Mu2e experiment, currently under construction at Fermilab, will search for neutrinoless  $\mu \rightarrow e$  conversion in the field of an aluminum atom. A clear signature of this charged lepton flavor violating two-body process is given by the monoenergetic conversion electron of 104.97 MeV produced in the final state.

An 8 GeV/c pulsed proton beam interacting on a tungsten target will produce the pions decaying in muons; a set of superconducting magnets will drive the negative muon beam to a segmented aluminum target where the stopped muons will eventually convert to electrons; a set of detectors will be used to both identify conversion electrons and reject beam and cosmic backgrounds.

The experiment will need 3-5 years of data-taking to achieve a factor of  $10^4$  improvement on the current best limit on the conversion rate.

After an introduction to the physics of Mu2e, we will report on the status of the different components of the experimental apparatus. The updated estimate of the experiment's sensitivity and discovery potential will be presented.

*The European Physical Society Conference on High Energy Physics (EPS-HEP2023)*

*21-25 August 2023*

*Hamburg, Germany*

---

\*[Mu2e Collaboration List, 2023](#).

\*Speaker

## 1. Introduction

The Mu2e experiment[1] is being assembled at Fermilab Muon Campus. Its main goal is the search for the charged-lepton flavour violating (CLFV) neutrino-less conversion of a negative muon into an electron (CE) in the field of an Aluminum nucleus:



Electrons produced by  $\mu$  conversions are nearly monochromatic with a peak energy of 104.97 MeV<sup>1</sup>.

The most stringent limit on this CLFV process has been set by the Sindrum II experiment in 2006: looking at the decay products from muons captured in a golden target it has set as 90% CL limit on the ratio between muon conversions and muon nuclear captures in Gold [2]:

$$R_{\mu e} = \frac{N(\mu \rightarrow e)}{N(\text{nuclear captures})} < 7 \cdot 10^{-13} \text{ (90\% CL)} \quad (2)$$

Mu2e goal is to improve by 4 order of magnitudes the Sindrum II sensitivity and eventually observe CLFV in the decays of the muons stopped in an Aluminum target. To achieve this major step in sensitivity Mu2e will benefit of a very intense muon beam and an almost background free detector. Thanks to its higher sensitivity Mu2e will be able to test some of the new theories that are predicting an  $R_{\mu e}$  value much higher than the  $10^{-49} \div 10^{-51}$  expected from the Standard Model[3].

## 2. Mu2e experimental apparatus

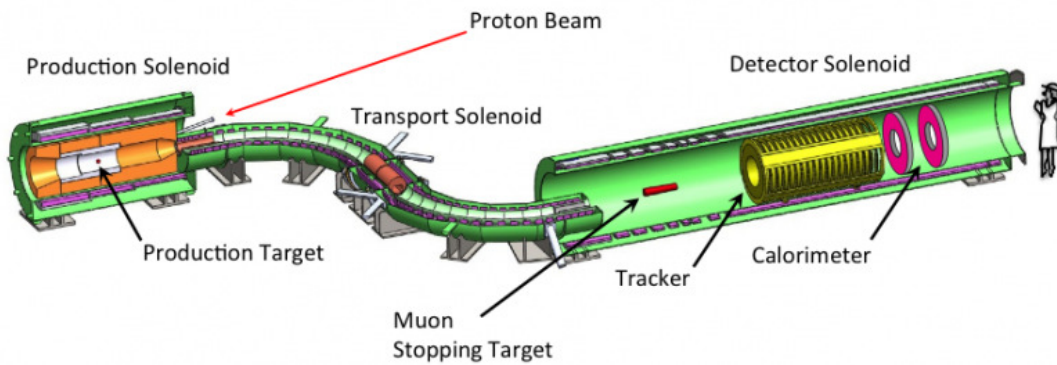


**Figure 1:** The Mu2e experimental apparatus.

Fig.1 shows the Mu2e experimental apparatus. A pulsed 8 GeV proton beam enters from the right to the Production Solenoid (PS) where a tungsten target is located. The graded magnetic field of the PS, varying from 4.5T to 2.5T, improves the collection efficiency of the S-shaped Transport Solenoid (TS) for the low momentum particles produced by the proton interactions on the production target. The TS provides a graded toroidal field (from 2.5T to 2T) that is used, together with a set of collimators, to choose the charge and the momentum of the particles that enter in the

<sup>1</sup>This is slightly less than the muon mass because of the nuclear recoil and the radiative corrections.

last solenoid, the Detector Solenoid (DS). In the normal configuration the collimator at the center of TS selects negative particles but for calibration purposes it can be rotated to select a positive beam. Two thin absorber windows, located at the entrance and in the middle of the TS, are used to suppress the background originating from antiprotons produced in the production target. The DS hosts the Aluminum target, segmented in 37 foils  $105\ \mu\text{m}$  thick (Fig.2), the tracker, the calorimeter and two polyethylene absorbers, inserted between the stopping target and the tracker, that reduce the radiation produced by the muon nuclear captures. The DS magnetic field decreases from 2T at the entrance to 1T in the tracker and calorimeter region.

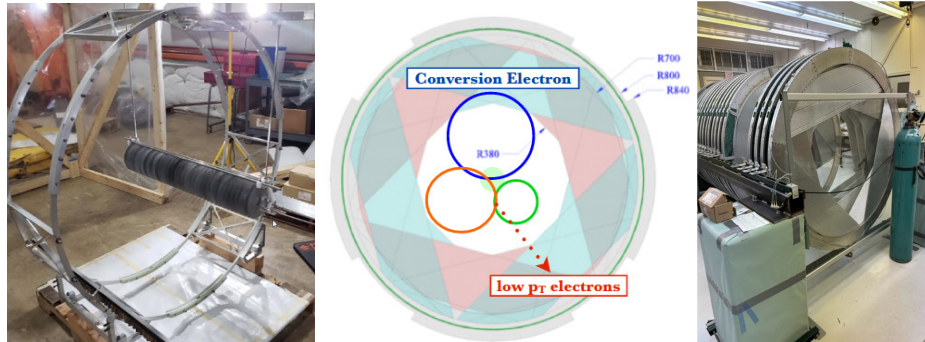


**Figure 2:** Left: the Aluminum Stopping Target. Center: tracker transverse view. Right: two tracker planes.

The straw tube tracker is made of  $\sim 21000$  tubes, with a diameter of 5 mm and a thin wall of  $15\ \mu\text{m}$  of mylar, filled with a 80%-20% Ar-CO<sub>2</sub> gas mixture. The anode is a  $25\ \mu\text{m}$  tungsten wire at 1450 V read by ADCs and TDCs. The straw tubes are arranged to form 18 anular stations with an inner radius of 380 mm and an outer radius of 700 mm. The anular shape makes the tracker insensitive to the particles with momentum lower than  $\sim 80\ \text{MeV}/c$ , in particular the low momentum beam particles and the vast majority of the electrons produced by the muon decays in the orbit (Fig.2). The transverse coordinate resolution measured on tracker prototypes is  $\sim 133\ \mu\text{m}$ . The reconstructed CE momentum distribution obtained by the simulation is nearly gaussian with a FWHM of  $0.96\ \text{MeV}/c$  and a small low momentum tail mainly due to energy losses.

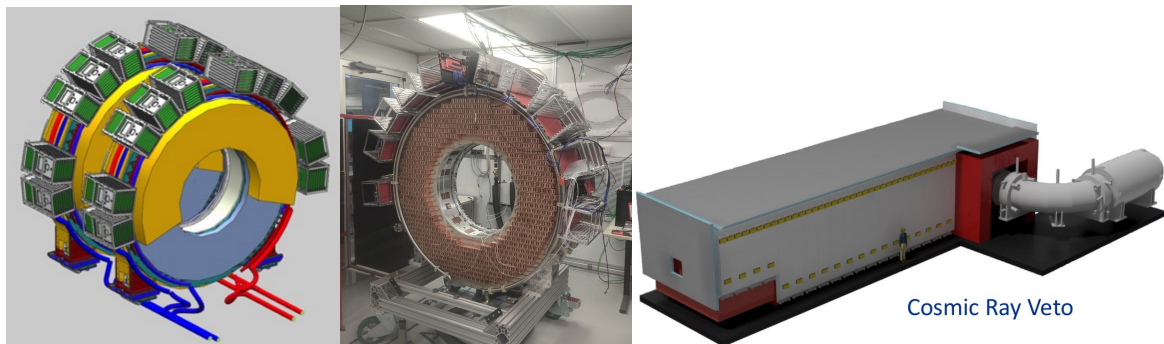


**Figure 3:** Left: ECAL disks. Center: first ECAL disk built. Right: CRV layout.

The electromagnetic calorimeter (ECAL) is made of 2 rings each containing 674 pure CsI

crystals (Fig.3). The rings inner radius is 374 mm and the outer one is 660 mm. Each crystal is read by 2 arrays of 6 SiPMs. A front end boards housing the preamplifier is attached to the back of the SiPM. The slow control mezzanine boards and the digitizer boards are hosted in crates placed on top of the rings. A test beam on a small scale prototype has demonstrated that ECAL energy ( $\sim 7\%$ ) and time resolution ( $\sim 230 \text{ ps}^2$ ) well satisfy the requirement for CE electrons identification[4].

The DS and the lower part of the TS are covered by a Cosmic Ray Veto (CRV, Fig. 3) system made of 4 layers of scintillators read by SiPM that provides a factor  $10^4$  rejection on charged cosmic particles.

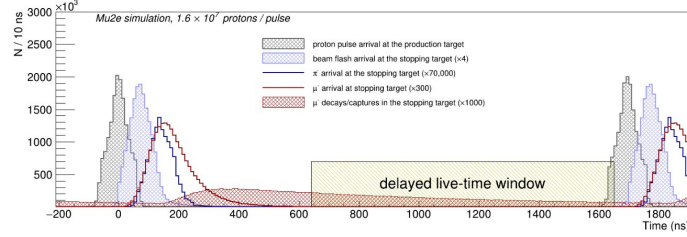


**Figure 4:** Pulsed proton beam structure.

The structure of the proton beam is shown in Fig.4. The choice of the time interval between two proton spills ( $\sim 1.7 \mu\text{s}$ ) has been driven by the muonic Al lifetime (864 ns). Data will be collected starting from 500 ns after the protons arrival to the production target, while the search for CE candidates will start about 200 ns later. Prompt backgrounds like the ones originated by the Radiative Pion Captures (RPCs) in the stopping target will be suppressed to a negligible level if the fraction of protons out of spill, called extinction factor, will be lower than  $10^{-10}$ . The current measurements of the accelerator line indicate an extinction factor of  $10^{-12}$ . This quantity will be measured by the Extinction Monitor detector located downstream of the production target.

### 3. Expected sensitivity for the Mu2e Run 1

Mu2e Run 1 is scheduled to start in 2026 and will end with the shutdown for the Proton Improvement Plan II (PIP-II) of Fermilab accelerator complex. This first run aims to improve by a factor  $10^3$  Sindrum II result and to study the detector systematics that can eventually be corrected before the start of the second run. For this reason part of this run will use a beam intensity reduced by one half, using one bunch per proton batch instead of two.

An intense simulation and analysis campaign has been performed to evaluate the sensitivity for muon conversions corresponding to  $6 \cdot 10^{16}$  stopped muons, that is the expected amount of data collected in Run 1, and using a realistic description of the experimental conditions based of the latest understanding of the accelerator and detector performances[5].

The main backgrounds come from cosmic rays eluding the CRV and from the muon decays in orbit. The RPC background can be efficiently suppressed by a time cut.

The final selection is given by the cuts on the event time and the particle reconstructed momentum indicated by the arrows in Fig. 5:  $640 < t < 1650 \text{ ns}$  and  $103.6 < p < 104.9 \text{ MeV}/c$ .

<sup>2</sup>This is a conservative estimate since it has been obtained using only one sensor per crystal.

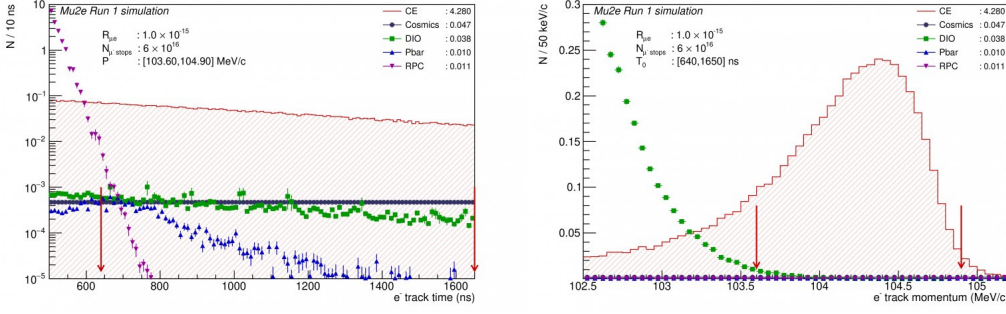


**Figure 5:** Time (left) and momentum (right) of candidate conversion electrons. The signal distributions correspond to  $R_{\mu e} = 10^{-15}$

Channel	Mu2e Run 1 Simulation results
SES	$2.4 \cdot 10^{-16}$
Cosmics	$0.046 \pm 0.010$ (stat) $\pm 0.009$ (syst)
DIO	$0.038 \pm 0.002$ (stat) $^{+0.025}_{-0.015}$ (syst)
Antiprotons	$0.010 \pm 0.003$ (stat) $+0.010$ (syst)
RPC	$0.010 \pm 0.002$ (stat) $^{+0.001}_{-0.003}$ (syst)
Total	$0.105 \pm 0.032$ (stat $\oplus$ syst)

**Table 1:** Mu2e Run 1 expected single event sensitivity (SES) and background levels[5].

These cuts have been optimized to achieve the best  $5\sigma$  discovery sensitivity. The final single event sensitivity and background levels are summarized in Tab.1[5].

Given the very low background level a  $5\sigma$  discovery will be claimed after observing just 5 events, corresponding to  $R_{\mu e} = 1.1 \cdot 10^{-15}$ . If no events will be observed the 90% CL limit will be set at  $R_{\mu e} = 6.2 \cdot 10^{-16}$ , that is more than a factor  $10^3$  improvement with respect to Sindrum II.

#### 4. Mu2e Run 2 and beyond

The second Mu2e run will start after the Fermilab accelerator shutdown for the proton beam upgrade that is expected to be completed by 2029. Thanks to an improved average beam intensity and a refined detector shielding that will profit of the Run 1 experience, Run 2 aims to achieve the final  $10^4$  improvement on CE sensitivity.

At the same time Mu2e will look for lepton number violating process:

$$\mu^- N(A, Z) \rightarrow e^+ N(A, Z - 2)$$

with a Run 1 SES on  $R_{\mu e^+} = 4 \cdot 10^{-16}$ . with more than a factor  $10^3$  improvement with respect to the current limit:  $R_{\mu e^+} < 1.7 \cdot 10^{-12}$  (90% CL, Sindrum II[6]). In this case the main background comes from the tail of the spectrum of the Radiative Muon Capture photons that will also be better constrained after Mu2e Run 1.

A Mu2e upgrade proposal, called Mu2e II, has been inserted in the Snow Mass white paper[7]: it aims to exploit the higher intensity and lower energy PIP-II proton beam to obtain a further factor 10 improvement with respect to Mu2e final result.

## 5. Summary

Mu2e construction is under way and on schedule to collect first physics data in 2026. The first run, before Fermilab accelerator shutdown, is expected to improve the Sindrum II limit by a factor  $10^3$ . A second run, expected to start in 2029, is expected to reach the final  $10^4$  improvement allowing to confirm or discard many Standard Model extensions predicting an enhancement of CLFV probability in muon conversion.

## 6. Acknowledgments

We are grateful for the vital contributions of the Fermilab staff and the technical staff of the participating institutions. This work was supported by the US Department of Energy; the Istituto Nazionale di Fisica Nucleare, Italy; the Science and Technology Facilities Council, UK; the Ministry of Education and Science, Russian Federation; the National Science Foundation, USA; the National Science Foundation, China; the Helmholtz Association, Germany; and the EU Horizon 2020 Research and Innovation Program under the Marie Skłodowska-Curie Grant Agreement Nos.734303, 822185, 858199, 101003460, and 101006726. This document was prepared by members of the Mu2e Collaboration using the resources of the Fermi National Accelerator Laboratory (Fermilab), a U.S. Department of Energy, Office of Science, HEP User Facility. Fermilab is managed by Fermi Research Alliance, LLC (FRA), acting under Contract No. DE-AC02-07CH11359.

## References

- [1] L. Bartoszek et al., *Mu2e Technical Design Report, Fermilab-TM-2594, Fermilab-DESIGN-2014-1, arXiv:1501.05241* (2014).
- [2] Wilhelm H. Bertl et al., *A Search for muon to electron conversion in muonic gold, Eur. Phys. J. C* **47** (2006) 337.
- [3] W. Altmannshofer et al., *Anatomy and Phenomenology of FCNC and CPV Effects in SUSY Theories, arXiv:0909.1333v2* (2010).
- [4] N. Atanov et al., *Electron beam test of the large area Mu2e calorimeter prototype*, in proceedings of *18th International Conference on Calorimetry in Particle Physics (CALOR 2018)*.
- [5] F. Abdi et al. (Mu2e collaboration), *Mu2e Run I Sensitivity Projections for the Neutrinoless  $\mu^- \rightarrow e^-$  Conversion Search in Aluminum, Universe* **9** (2023) *1, 54, Fermilab-PUB-22-749-PPD, arXiv:2210.11380* (2022).
- [6] J. Kaulard et al., *Improved limit on the branching ratio of  $\mu^- \rightarrow e^+$  conversion on titanium, Phys.Lett.B* **422** (1998) 334-338
- [7] K. Byrum et al., *Mu2e-II: Muon to electron conversion with PIP-II /arXiv.2203.07569*